Refractive index and oscillator parameters in $TlGaS_2$, $TlGaSe_2$ and $TlInS_2$ layered crystals

N. M. GASANLY
Department of Physics, Middle East Technical University, 06531 Ankara, Turkey

The optical properties of $TlGaS_2$, $TlGaSe_2$, and $TlInS_2$ crystals have been investigated through the transmission and reflection measurements at room temperature in the wavelength range of 400–1100 nm. These measurements allowed determination of spectral dependence of the refractive index for all crystals studied. The dispersion of the refractive index is discussed in terms of the Wemple-DiDomenico single-effective-oscillator model. The refractive index dispersion parameters: the oscillator energies, the dispersion energies, and the zero-frequency dielectric constants and refractive indices were determined.

(Received December 9, 2010; accepted January 26, 2011)

Keywords: Optical properties, Refractive index, Semiconductors

1. Introduction

Information about the spectral dependence of optical parameters such as refractive index, dielectric constant, reflectivity and absorption coefficients are essential in the characterization of materials that are used in the fabrication of optoelectronic devices. The family of crystals designated with the chemical formula $TlBX_2$ (where B = In or Ga, X = S, Se or Te) are known as thallium dichalcogenides. Members of this family have both layered ($TlGaS_2$, $TlGaSe_2$, $TlInS_2$) and chain ($TlInSe_2$, $TlInTe_2$, $TlGaTe_2$) structures [1,2]. Stacking of the atoms in $TlGaS_2$, $TlGaSe_2$, and $TlInS_2$ layered crystals is arranged in a form of two twisted anionic layers with the week bonded Tl^{1+} cations located in the trigonal cavities between them. Therefore, the crystals consist of separate layers with the strong bonding between atoms within the layer and the weak bonding between the layers.

The optical and electrical properties of $TlGaS_2$, $TlGaSe_2$, and $TlInS_2$ layered crystals were studied in Refs. [3–7]. These crystals are useful for optoelectronic applications as they have high photosensitivity in the visible range of the spectra and a wide transparency range of 0.5–14.0 μm [8]. In the past, a large number of studies were accumulated about the fundamental optical absorption in the $TlGaS_2$, $TlGaSe_2$, and $TlInS_2$ crystals [9–19]. Namely, the fundamental absorption edge was reported to be formed by the indirect and the direct transitions with room temperature energies varying over the large ranges: E_{gi} = 2.35–2.46 eV and E_{gd} = 2.38–2.64 eV ($TlGaS_2$), E_{gi} = 1.83–2.13 eV and E_{gd} = 2.08–2.23 eV ($TlGaSe_2$), E_{gi} = 2.24–2.33 eV and E_{gd} = 2.33–2.40 eV ($TlInS_2$), respectively. It should be noted that the most transmission measurements were carried out on the samples with the thickness in the range of 40-420 μm.

In this paper, we present the results of the transmission and reflection measurements performed on the $TlGaS_2$, $TlGaSe_2$, and $TlInS_2$ layered crystals in order to derive the refractive index. The refractive index dispersion data were analyzed using the Wemple-DiDomenico single-effective-oscillator model. As a result, the oscillator energy E_{so}, dispersion energy E_d and zero-frequency refractive index n_0 were determined for studied crystals. The determination of these optical constants is expected to expand the available physical information.

2. Experimental details

Single crystals of $TlGaS_2$, $TlGaSe_2$, and $TlInS_2$ were grown by the Bridgman method from a stoichiometric melt of starting materials sealed in the evacuated (10^{-5} Torr) and carbon coated silica tubes (10 mm in diameter and about 25 cm in length) with a tip at the bottom in our crystal growth laboratory. The resulting ingots of the $TlGaS_2$, $TlGaSe_2$, and $TlInS_2$ single crystals (yellow-green, red and orange in color, respectively) had no cracks and voids on the surface. The chemical composition of crystals studied was determined by the energy dispersive spectroscopic analysis using JSM-6400 electron microscope. The atomic composition ratio of the samples was estimated as (25.4 : 25.6 : 49.0), (25.4 : 25.2 : 49.4) and (25.6 : 25.2 : 49.2) for the $TlGaS_2$, $TlGaSe_2$, and $TlInS_2$, respectively. The samples for the optical measurements were taken from the middle part of the ingots. The freshly cleaved platelets (along the layer plane (001)) were mirror-like. That is why no further polishing and cleaning treatments were required.

The transmission and the reflection measurements were carried out at room temperature in the 400–1100 nm wavelength region with a “Shimadzu” UV–1201 model spectrophotometer. The transmission measurements were

done under the normal incidence of light with the polarization direction along the (001) plane, which is perpendicular to the ***c***-axis of the crystal. For the reflection experiments, the specular reflectance measurement attachment with 5° incident angle was used. The measured reflections were compared against a protected silver mirror "Thorlabs PF 10-03-P01". The resolution of the spectrophotometer was 5 nm.

3. Results and discussion

Figs. 1 and 2 present the transmittance (T) and the reflectivity (R) spectra of the $TlGaS_2$, $TlGaSe_2$, and $TlInS_2$ crystals registered in the wavelength (λ) range from 400 to 1100 nm, respectively. The absorption coefficient α and the refractive index n were calculated using the following relations [20]

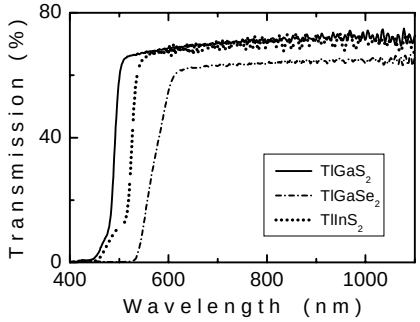

Fig. 1. The spectral dependencies of the transmission for $TlGaS_2$, $TlGaSe_2$, and $TlInS_2$ crystals at T = 300 K.

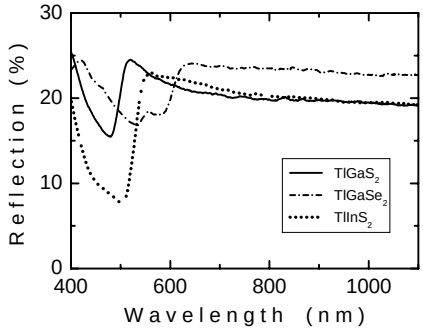

Fig. 2. The spectral dependencies of reflection for $TlGaS_2$, $TlGaSe_2$, and $TlInS_2$ crystals at T = 300 K.

$$\alpha = \frac{1}{d}\ln\left\{\frac{(1-R)^2+\left[(1-R)^4+4R^2T^2\right]^{1/2}}{2T}\right\} \qquad (1)$$

$$n = \frac{1+R}{1-R}+\left[\frac{4R}{(1-R)^2}-\left(\frac{\alpha\lambda}{4\pi}\right)^2\right]^{1/2}, \qquad (2)$$

where d is the sample thickness.

The reflection measurements were carried out using the specimens with natural cleavage planes and the thickness such that $\alpha d >> 1$. The sample thickness was then reduced (by repeated cleaving using the transparent adhesive tape) until it was convenient for measuring the transmission spectra. The thickness of the sample was determined through the transmission interference fringes at the wavelengths slightly longer than the intrinsic absorption edge, where the sample has relatively high transmission values (Fig. 1). We evaluated the thickness of the sample by measuring the wavelengths at which two adjacent transmission maxima occur [21]

$$d = \frac{\lambda_1\lambda_2}{2n(\lambda_2-\lambda_1)}. \qquad (3)$$

The long wavelength values of the refractive index n = 2.55 ($TlGaS_2$), n = 2.82 ($TlGaSe_2$), and n = 2.58 ($TlInS_2$), found from the reflection measurements, was used to determine the thickness of the sample, which turned out to be about 10 μm for transmission measurements in most of the cases.

Figs. 3 displays the dependencies of the refractive indices n on the wavelength that were determined employing Eqs. (1) and (2). It is possible to observe that the refractive indices in the energy region of $h\nu < E_g$ gradually decrease from 2.96 to 2.55 ($TlGaS_2$), 2.92 to 2.82 ($TlGaSe_2$), and 2.85 to 2.58 ($TlInS_2$) with increasing wavelength up to 1100 nm. The dispersive refractive index data in $h\nu < E_g$ range were analyzed according to the single-effective-oscillator model proposed by Wemple and DiDomenico [22, 23]. The refractive index is related to the photon energy through the relationship

$$n^2(h\nu) = 1 + \frac{E_{so}E_d}{E_{so}^2-(h\nu)^2}, \qquad (4)$$

where E_{so} is the single oscillator energy and E_d is the dispersion energy. Plotting $(n^2-1)^{-1}$ versus $(h\nu)^2$ allows the determination of the oscillator parameters by fitting a linear function to the lower energy data range. The fittings of the above reported function are presented in Figs. 4(a)-4(c). The zero-frequency refractive index n_0 is estimated from Eq. (4), i.e. according to the expression $n_0^2 = 1+\frac{E_d}{E_{so}}$.

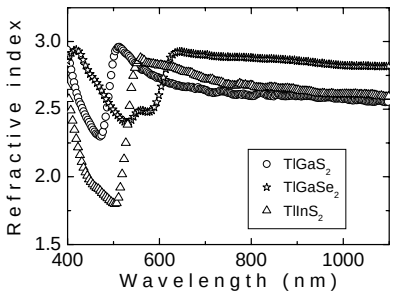

Fig. 3. The dependencies of refractive indices on the wavelength for $TlGaS_2$, $TlGaSe_2$, and $TlInS_2$ crystals.

The values of the parameters E_{s0} and E_d were calculated from the slope and the intersection with *y*-axis of the straight lines (Figs. 4(a)-4(c)) as 4.51 and 24.02 eV ($TlGaS_2$), 4.96 and 34.02 eV ($TlGaSe_2$), and 6.02 and 33.32 eV ($TlInS_2$). Furthermore, the values of the zero-frequency dielectric constants $\varepsilon = n_0^2 =$ 6.35, 7.84, and 6.55 and the refractive indices n_0 = 2.51, 2.80, and 2.56 were evaluated by means of Eq. (3) for the $TlGaS_2$, $TlGaSe_2$, and $TlInS_2$ crystals, respectively. The oscillator energy E_{so} is an "average" energy gap and, to fair approximation, it is associated empirically with the lowest direct band gap E_{gd} by the relation $E_{so} \approx 2.0\ E_{gd}$ [24,25]. The ratio E_{so}/E_{gd}, determined in this study, was found to be 1.79 ($TlGaS_2$), 2.17 ($TlGaSe_2$), and 2.24 ($TlInS_2$).

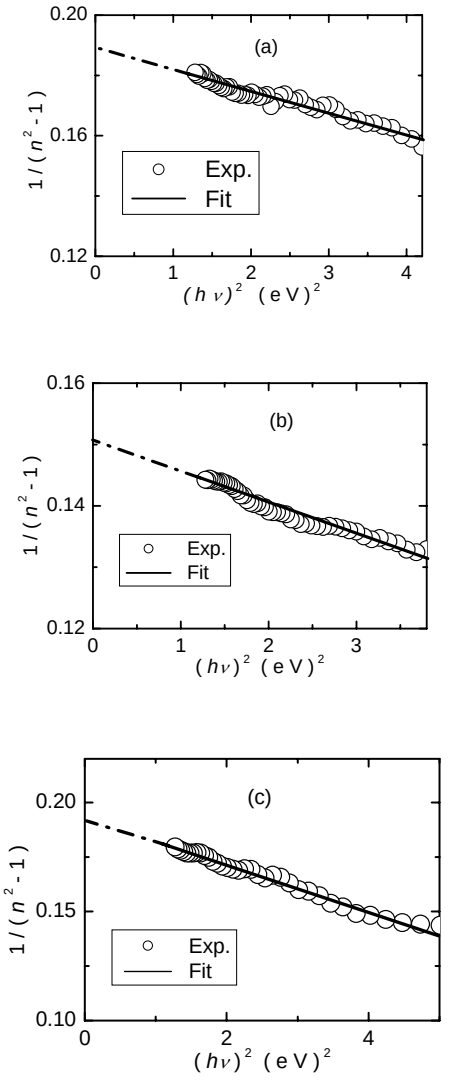

Fig. 4. Plots of $(n^2 - 1)^{-1}$ *versus* $(h\nu)^2$*: (a)* $TlGaS_2$*, (b)* $TlGaSe_2$*, and (c)* $TlInS_2$*. The solid lines represent the fits using Eq. (3).*

At this point, it is worthwhile to compare the dispersive refractive indices presented above with those previously reported for the $TlGaS_2$, $TlGaSe_2$, and $TlInS_2$ crystals [26-29]. In this study, the determined values of the refractive indices, corresponding to the λ = 700 nm (which was the only common wavelength chosen for the comparison with the results of the other studies), were found to be 2.65 ($TlGaS_2$), 2.91 ($TlGaSe_2$), and 2.70 ($TlInS_2$). The values of the refractive indices obtained in literature for the same wavelength were equal to 2.54 [3] and 2.63 [26] ($TlGaS_2$), 2.82 [3], 2.88 [27], and 2.38 [28] ($TlGaSe_2$), and 2.54 [3] and 2.68 [29] ($TlInS_2$). As a whole, the obtained picture is consistent with the well-known fact that refractive index and the energy gap are inversely related to each other [20]. Particularly, for the $TlGaSe_2$ crystal, which has the smallest band gap energy among the studied materials, the refractive index shows the largest value (2.91).

It is possible to observe from Fig. 4(a) that the refractive index of the $TlGaS_2$ crystals is steeply increasing as the photon energy approaches the energy band gap. Similar but less pronounceable behavior of *n* with the photon energy is demonstrated by the $TlInS_2$ crystals (Fig. 4(c)). At the same time, refractive index of the $TlGaSe_2$ crystals does not show strong dispersion at least to an extent given by the obtained data (Fig. 4(b)).

4. Conclusions

The transmission and reflection spectra of the $TlGaS_2$, $TlGaSe_2$, and $TlInS_2$ crystals were measured over the spectral region of 400–1100 nm to derive the refractive index. The dispersion of the refractive index is analyzed using the concept of the Wemple–DiDomenico single-effective-oscillator model. As a result, the oscillator and the dispersion energies, and the zero-frequency refractive index were determined.

Acknowledgement

The author is grateful to Dr. K. Goksen and I. Guler for their assistance.

References

[1] K. A. Yee, A. Albright, J. Am. Chem. Soc. **113**, 6474 (1991).
[2] A.M. Panich, J. Phys.: Condens. Matter **20**, 293202 (2008).
[3] Y. Shim, W. Okada, K. Wakita, N. Mamedov, J. Appl. Phys. **102**, 083537 (2007).
[4] A. Kato, M. Nishigaki, N. Mamedov, M. Yamazaki, S. Abdullaeva, E. Kerimova, H. Uchiki, S. Iida, J. Phys. Chem. Sol. **64**, 1713 (2003).

[5] T. D. Ibrahimov, I. I. Aslanov, Solid State Commun. **123**, 339 (2002).
[6] I. M. Ashraf, M. M. Abdel-Rahman, A. M. Badr, J. Phys. D: Appl. Phys. **36**, 109 (2003).
[7] Y. Rud, V. Rud, M. Morohashi-Yamazaki, H. Uchiki, N. Mamedov, Inst. Phys. Conf. Ser. **152**, 967 (1998).
[8] K. R. Allakhverdiev, Solid State Commun. **111**, 253 (1999).
[9] M. Hanias, A. Anagnostopoulos, K. Kambas, J. Spyridelis, Physica B **160**, 154 (1989); Mat. Res. Bull. **27**, 25 (1992).
[10] N. Kalkan, M. P. Hanias, A. Anagnostopoulos, Mat. Res. Bull. **27**, 1329 (1992).
[11] S. Duman, B. Gurbulak, Phys. Scripta **72**, 82 (2005); **77**, 025702 (2008).
[12] V. Grivickas, V. Bikbajevas, P. Grivickas, Phys. Status Solidi B **243**, R31 (2006).
[13] I. M. Ashraf, J. Phys. Chem. **108**, 10765 (2004).
[14] O. Karabulut, M. Parlak, G. M. Mamedov, J. All. Comp. **429**, 50 (2007).
[15] S. Kashida, Y. Yanadori, Y. Otaki, Y. Seki, A.M. Panich, Phys. Status Solidi A **203**, 2666 (2006).
[16] S. R. Samedov, O. Baykan, A. Gulubayov, Int. J. Inf. Millimet. Waves **25**, 735 (2004).
[17] A. M. Akhmedov, A. E. Bakhyshov, A. A. Lebedev, M.A. Yakobson, Sov. Phys. Semicond. **12**, 299 (1978).
[18] H. Uchiki, D. Kanazawa, N. Mamedov, S. Iıda, J. Luminescence **87-89**, 664 (2000).
[19] G. A. Gamal, Semicond. Sci. Technol. **13**, 185 (1998).
[20] J. I. Pankove, Optical Processes in Semiconductors, Prentice-Hall , New Jersey (1971).
[21] T. S. Moss, G.J. Burrell, B. Ellis, Semiconductor Opto-electronics, Butterworths, London (1973).
[22] S. H. Wemple, M. DiDomenico, Phys. Rev. B **3**, 1338 (1971).
[23] S. H. Wemple, M. DiDomenico, Phys. Rev. Lett. **23**, 1156 (1969).
[24] K. Tanaka, Thin Solid Films 66, 271 (1980).
[25] F. Yakuphanoglu, A. Cukurovali, I. Yilmaz, Physica B 351, 53 (2004); Physica B **353**, 210 (2004).
[26] A. F. Qasrawi, N.M. Gasanly, Phys. Status Solidi A **202**, 2501 (2005).
[27] J. A. Kalomiros, N. Kalkan, M. Hanias, A. N. Anagnostopoulos, K. Kambas, Solid State Commun. **96**, 601 (1995).
[28] M. M. El-Nahass, M. M. Salam, S. A. Rahman, E. M. Ibrahim, Solid State Sci. **8**, 488 (2006).
[29] J. A. Kalomiros, A. N. Anagnostopoulos, Phys. Rev. B **50**, 7488 (1994).

*Corresponding author: nizami@metu.edu.tr